Random sequential adsorption of objects of decreasing size

Oleksandr Gromenko and Vladimir Privman
Department of Physics, Clarkson University, Potsdam, New York 13699-5721, USA
(Received 25 September 2008; published 7 January 2009)

We consider the model of random sequential adsorption, with the depositing objects, as well as those already at the surface, decreasing in size according to a specified time dependence, from a larger initial value to a finite value in the large-time limit. Numerical Monte Carlo simulations of two-dimensional deposition of disks and one-dimensional deposition of segments are reported for the density-density correlation function and gap-size distribution function, respectively. Analytical considerations supplement numerical results in the one-dimensional case. We investigate the *correlation hole*—the depletion of correlation functions near contact and, for the present model, their vanishing at contact—that opens up at finite times, as well as its closing and reemergence of the logarithmic divergence of correlation properties at contact in the large-time limit.

DOI: 10.1103/PhysRevE.79.011104 PACS number(s): 02.50.−r, 68.43.Mn, 05.10.Ln, 05.70.Ln

I. INTRODUCTION

The random sequential adsorption (RSA) model has attracted a lot of attention and has a long history [1–4]. It finds applications, e.g., [1–9] in many fields, ranging from surface science to polymers, biology, device physics, and physical chemistry. Traditionally, the RSA model assumed that particles are transported to a substrate which is a continuous surface or a lattice, the latter convenient for numerical simulations. Upon arrival at the surface the particles are irreversibly deposited, but only provided they do not overlap previously deposited objects. Otherwise, the deposition attempt is rejected and the arriving particle is assumed transported away from the substrate. The original RSA model studies were largely motivated by surface deposition of micrometer-sized objects, such as colloid particles. Particles of this size are typically not equilibrated on the surface, and are larger than most surface features and the range of most of the particle-particle and particle-surface interactions. Various generalizations of the basic RSA model have been considered in the literature, e.g., [8–29] including "soft" rather than hard-core particle-particle interactions, as well as relaxation by motion of particles on the surface.

Recently, experimental surface-deposition work has expanded to nanosized particles and submicrometer-feature-patterned (ultimately, nanopatterned) surfaces [30–33]. The added control of the particle and surface "preparation" as part of the deposition process could allow new functionalities in applications, and therefore it has prompted new research efforts. Specifically, deposition on surfaces prepared with patterns other than regular lattices was studied [24,25], motivated by new experimental capabilities in surface patterning. Another development involved a study [8,15,17] of one-dimensional deposition of segments that, after attachment to the substrate, can shrink or expand, motivated by potential applications, e.g., in device physics [10,11].

The motivation for our present work has been the newly emerging experimental capability [34,35] of depositing polymer "blobs" (or polymer-coated particles) the size of which can be modified by changing the solution chemistry: Approximately spherical particles can be deposited in a process whereby their effective size (including the interaction radius) is varied on a time scale comparable to that of the deposit formation. The size of both the particles in solution and those already deposited will thus vary with time, in a controllable fashion.

For particle deposits formed on prepatterned surfaces, an interesting property is suggested by experiments [36–42], and theoretically verified [24,25]: They acquire semiordering properties "imprinted" by the substrate, as quantified by the development of peaks in the two-particle correlation. However, as in the original irreversible RSA model, there remains a significant peak at particle-particle contact, which, for deposition continuing indefinitely, at infinite times becomes a weak singularity [43,44]. This tendency of particles to form clumps is undesirable mostly because many nanotechnology applications rely on nanoparticles utilized in isolation, or simply being kept away from each other to avoid merging. In this work, we establish that deposition of particles of varying, specifically, *decreasing* size, can yield deposits without clumping, by opening a "correlation hole," i.e., a property of depletion of two-particle correlations near contact, as defined in other fields, e.g., [45–50]. In our case, the correlation functions studied actually vanish at contact for finite deposition times.

The outline of this paper is as follows. In Sec. II, we consider the two-dimensional (2D) deposition of shrinking disks in a plane. The model is defined and then a two-point density-density correlation function is studied by numerical Monte Carlo simulations. In Sec. III, we present both numerical and analytical analyses of the one-dimensional (1D) deposition of shrinking segments on a line. Our 1D study focuses on the gap-density distribution function. A brief summary is offered at the end of Sec. III.

II. DEPOSITION OF DISKS ON A TWO-DIMENSIONAL SUBSTRATE

A. Definition of the model

In this section, we introduce the model for the most relevant geometry for possible applications: The 2D RSA model of deposition of disks of diameters $D(t)$ on an initially empty planar substrate. A 1D model of deposition of seg-

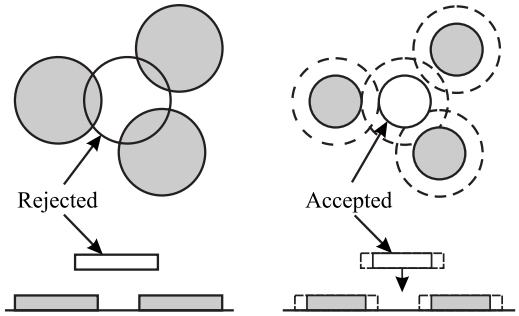

FIG. 1. Left panel: Deposition attempts in 2D and 1D that are rejected due to particle overlap. Right: A situation at a later time at which the same deposition attempts would succeed due to particle shrinkage.

ments on a line provides additional insight into the problem and will be considered in the next section.

As usual in RSA, we assume that disks are transported to the surface with the resulting deposition attempt flux R per unit area and unit time t. A disk adsorbs only if it does not overlap a previously deposited one. The diameter of all the disks, those already on the surface and those arriving, is a decreasing function of time, $\dot{D}(t)<0$, varying between two nonzero values $D(0)>D(\infty)>0$. For the 2D model, we carried out numerical Monte Carlo simulations to estimate the particle-particle pair correlation function that describes the relative positioning of the disks with respect to each other. It is defined as the ratio of the number of particle centers N at distances from r to $r+dr$ from a given particle's center, normalized per unit area and per the deposit density ρ,

$$P_2(r,t) = \frac{N(r,dr,t)}{(2\pi r\, dr)\rho(t)}. \tag{1}$$

In studies of RSA, $\rho(t)$ is usually a quantity of interest. It grows linearly for short times and reaches a jamming-limit value, which is less than close packing, for large times. In the latter regime the approach to the jamming coverage on a continuum substrate is described by a power law [43,44,51]. However, in our present study we found by numerical simulations no new interesting features for $\rho(t)$ for the considered time dependences of the disk diameters (specified below). Therefore, we focus our presentation on the correlation function, and specifically its properties near particle contact, at $r \simeq D(t)$.

The model is illustrated in Fig. 1. We note that if the disks shrink too fast as compared to the time scale of the buildup of the deposited layer, which is of order $\sim 1/RD^2$, then the problem will be reduced to that of simply depositing smaller disks. On the other hand, if the disks shrink too slowly as compared to the time scale $\sim 1/RD^2$, then the depletion of the correlations at contact will be trivially attributable to disk shrinkage alone. We are interested in the interplay of two effects: The decreasing disk size enlarges voids between already deposited disks. At the same time this process increases the rate of successful disk deposition events, which reduce voids between disks. Given that numerical simulations for this problem are quite demanding, we report results for the following time dependence for the disk radius:

$$D(t) = D(\infty)\{1 + \exp[-RD^2(\infty)t]\}. \tag{2}$$

We also studied numerically the cases

$$D(t) = D(\infty)\left(1 + \frac{1}{\ln[e + RD^2(\infty)t]}\right), \tag{3}$$

$$D(t) = D(\infty)\left(1 + \frac{1}{1 + RD^2(\infty)t}\right), \tag{4}$$

and found qualitatively similar results.

B. Numerical results

Let us now briefly outline the numerical procedure used in our Monte Carlo simulations. In order to calculate the correlation function $P_2(r,t)$, we have to generate a distribution of deposited objects. We used periodic boundary conditions and system sizes $L \times L = 500D(\infty) \times 500D(\infty)$. The xy coordinates of the center of the next disk that makes a deposition attempt were randomly generated. If the disk does not overlap any of the previously deposited ones, then it is deposited. The total number of deposition attempts is thus equal to $RL^2\Delta t$ for a physical time interval Δt. All our data presented below were averaged over 100 independent Monte Carlo runs.

We point out that there exist algorithms for studying RSA at large times [52], specifically designed to account for the fact that isolated residual voids (defined as landing areas for particle centers for allowed depositions) then evolve independently. However, in our case we were primarily interested in intermediate times. Furthermore, as disks already adsorbed on the surface shrink, all the voids increase and some might merge to form larger voids. Therefore, we used the straightforward algorithm described in the preceding paragraph.

Our main result is illustrated in Fig. 2. The correlation function introduced earlier is plotted for several times, which are multiples of the characteristic process time scale

$$\tau = 1/RD^2(\infty). \tag{5}$$

At finite times the correlation function has a peak at a value $r/D(\infty)>1$, and actually vanishes at the disk contact, when $r=D(t)$. This correlation hole behavior is in contrast with the ordinary RSA, e.g., [7,51], for which the correlation function, instead of developing a peak close to contact, actually increases as the disk separation decreases toward contact, and reaches, for finite times, a constant, nonzero value at contact. The correlation hole property represents the formation of a certain degree of short-range ordering in the system, and specifically avoidance of particle clumping.

In the limit $t \to \infty$, the correlation hole closes and the correlation function seems to develop a weak divergence as $r \to D(\infty)$. In fact, for constant disk diameters, this property has been studied by asymptotic analytical arguments [44] and numerically [7,51]: The weak logarithmic divergence of the correlation function of RSA at contact, is not easy to quantify numerically, and our data were not accurate enough

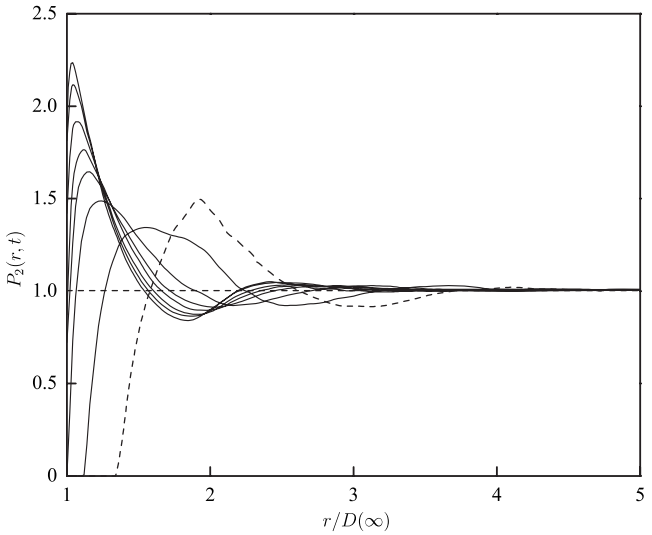

FIG. 2. Time evolution of the correlation function in deposition of disks with diameters shrinking according to Eq. (2). The dashed line corresponds to $t=\tau$. The solid lines with increasing peak values at $r/D(\infty)$ approaching 1 correspond, respectively, to $t=2\tau$, 4τ, 6τ, 8τ, 12τ, 18τ, and 24τ.

to study this limit for shrinking-diameter disk deposition by directly estimating $P_2(r,\infty)$. However, the time dependence of the peak values in Fig. 2 follows a logarithmic divergence as t increases, as shown in Fig. 3. This is reminiscent of a similar logarithmic divergence predicted [44] for the values of $P_2(D,t)$ at contact ($r=D$) for fixed-D RSA.

The formation of the finite-time correlation hole at disk contact was observed also for the nonexponential disk-diameter time dependences defined in Eqs. (3) and (4); see Fig. 4. This property of the correlation function is qualitatively similar for all three time-dependence protocols studied. However, we did not study larger time values for the nonexponential time dependences.

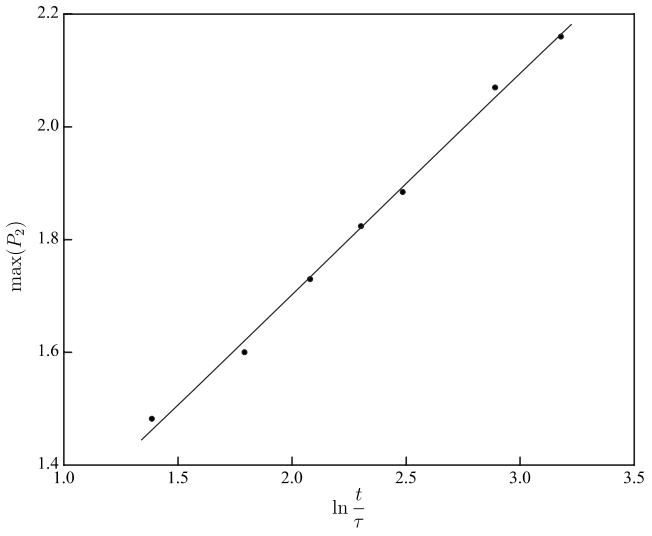

FIG. 3. Time dependence of the peak values of the correlation function, demonstrating the expected logarithmic divergence as $t\to\infty$. The least-squares fit of the peak values, shown here for times $t=4\tau,6\tau,8\tau,10\tau,12\tau,18\tau$, and 24τ, yields the slope of the solid line as 0.37 ± 0.02 (but note a comment in Sec. III C below regarding the low reliability of this "error-bar" estimate).

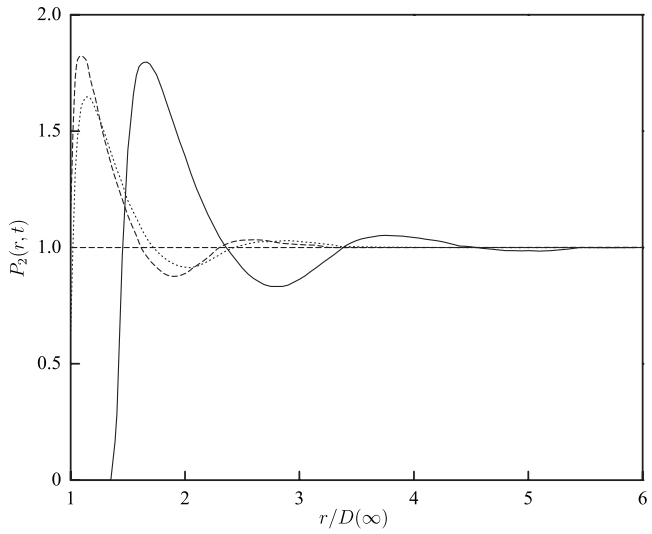

FIG. 4. Correlation function for $t=10\tau$, in deposition of disks with diameters shrinking according to Eq. (2), dashed line; Eq. (3), solid line; and Eq. (4), dotted line.

III. DEPOSITION OF SEGMENTS ON A LINE

A. Numerical results

In this section we report numerical results for the 1D deposition of segments on an initially empty line. The segment length is a function of time, $\ell(t)$, monotonically decreasing from $\ell(0)$ to $\ell(\infty)$. Our numerical results in 1D were obtained for the exponential time dependence similar to the 2D case,

$$\ell(t)=\ell(\infty)\{1+\exp[-R\ell(\infty)t]\}. \tag{6}$$

We denote the number of deposition attempts per unit time per unit length (the flux) by R. The arriving segments are adsorbed only if they do not overlap any previously deposited ones; see Fig. 1. The quantity of interest is the gap density distribution function $G(x,t)$: The density of gaps (measured between the ends of the nearest-neighbor deposited segments) of length between x and $x+dx$ at time t is $G(x,t)dx$. The density of deposited segments at time t, which in 1D equals the density of gaps, is given by

$$n(t)=\int_0^\infty G(x,t)dx. \tag{7}$$

Our numerical simulations followed the same procedure as in 2D. In 1D, we used periodic boundary conditions and system sizes $10\,000\ell(\infty)$. The time scale [cf. Eq. (5)], was redefined for 1D,

$$\tau\equiv 1/R\ell(\infty). \tag{8}$$

Our results, shown in Fig. 5, represent averages over 10 000 independent Monte Carlo runs. One can see that the gap density distribution function is a smooth function of x for

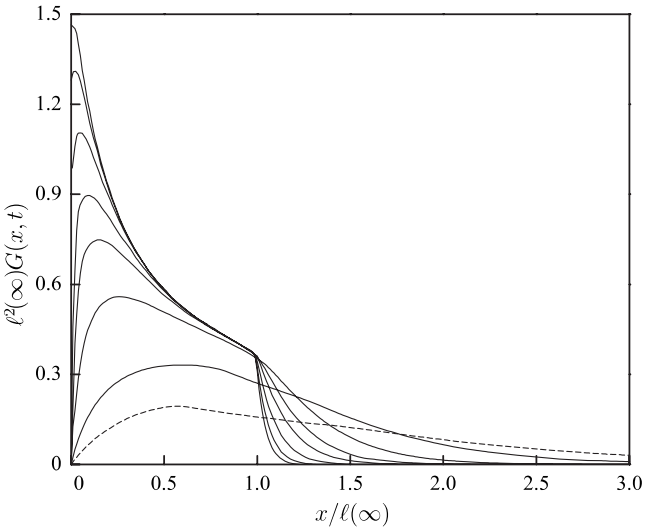

FIG. 5. Time evolution of the dimensionless gap-size distribution function $\ell^2(\infty)G(x,t)$ for segments with length shrinking according to Eq. (6). The dashed line corresponds to $t=\tau$. The solid lines with increasing peak values at $x/\ell(\infty)$ eventually approaching 0, correspond, respectively, to $t=2\tau,4\tau,6\tau,8\tau,12\tau,18\tau$, and 24τ.

finite times t, and for larger times it develops a pronounced peak at $x<\ell(t)$ approaching $x=0$. However, at $x=0$ for finite times there is a correlation hole. In the large-time limit, $G(x,t\to\infty)$ appears to develop a step at $x=\ell(\infty)$, as well as a divergence at $x=0$. These properties will be further discussed in the next two sections.

B. Analytical considerations

In this section, we will consider an analytical kinetic equation approach to the 1D deposition problem. This will allow us to elucidate the origin of the correlation hole at $x=0$. Kinetic equations, in closed form, or hierarchies of them, for RSA can be formulated for the gap density distribution function as well as for several other correlation-function-type quantities. They have been widely used for deriving exact results and low-density approximation schemes; see reviews in [1–4]. For the present problem, we have

$$\frac{\partial G(x,t)}{\partial t} = -R\theta(x-\ell(t))[x-\ell(t)]G(x,t) + 2R\int_{x+\ell(t)}^{\infty} G(y,t)dy + \dot{\ell}(t)\frac{\partial G(x,t)}{\partial x}. \qquad (9)$$

Here the first term represents the destruction of gaps of length x by segment deposition, with $\theta(\cdots)$ denoting the standard step function, which vanishes for negative arguments and is 1 for positive arguments. The second term represents the creation of gaps of length x due to deposition of segments landing in larger gaps of size $y>x+\ell(t)$. The last term describes the increasing size of all the gaps as a result of segment shrinkage. Note that the case $\dot{\ell}(t)=0$ is exactly solvable [53], and we will be using some of the exact results in the next section. For large x, we obviously have the boundary condition $G(x\to\infty,t>0)=0$ for Eq. (9). The following discussion explores the form of the boundary condition at the small-x side of the distribution.

There are two kinetic processes that alter gap lengths in our problem. First, deposition of segments can reduce the length by $\ell(t)$. This process can generate very small, positive gap lengths ϵ from available gaps of sizes $\ell(t)+\epsilon$. At the same time, the second process, that of segment shrinkage, causes all gap lengths to "drift" toward larger positive values with velocity $-\dot{\ell}(t)$. These two kinetic processes determine the evolution of the gap-length distribution $G(x,t)$ from its initial value $G(x,0)$. While our numerical simulations were for $G(x,0)=0$, we note that in principle one can generate other translationally invariant initial distributions by an appropriate preparation of the initial state. In fact, one can even prepare initial distributions that extend to small *negative* gap lengths. This entails allowing overlaps for the segments initially placed on the line, but not for those depositing later. If the segments are ordered according to their center-point positions, and each gap is measured as a consecutive center-point distance minus $\ell(t)$, then the initial-distribution overlaps, even if some are multi-segmented, can be unambiguously counted as negative gaps. The two kinetic processes will then remain the same: Gaps larger than $\ell(t)$ can be shortened due to deposition events, while at the same time *all* the gaps (positive, zero, negative) also increase toward positive values, due to segment shrinkage.

The above considerations suggest that Eq. (9) strictly speaking should be mathematically considered for $-\infty<x<\infty$. An attempt to limit it to $0\leqslant x<\infty$, and also use moment definitions, such as the zeroth-order moment Eq. (7), with integration over $0\leqslant x<\infty$, may in general yield wrong results: Neglecting the "flow of length" from the negative-x values may violate length conservation. However, in our case, specifically for the initial condition $G(x,0)=0$ [and with nonvanishing $\ell(t)$ for all t, including in the $t\to\infty$ limit, which avoids a possible singular limit], it is obvious that the problem should be definable with a boundary condition at $x=0$ because all the kinetics of the process occurs in $0\leqslant x<\infty$. Indeed, together with the zeroth-order moment, the first-order moment of the distribution can be used to determine the applicable boundary condition directly from length conservation,

$$\ell(t)n(t) + \int_0^{\infty} xG(x,t)dx = 1. \qquad (10)$$

Here the first term is the density of the covered area, whereas the second term is the density of the uncovered area. Both densities are "per unit length" in 1D, and therefore they sum up to 1.

The derivation proceeds as follows. We take the time derivative of Eq. (10),

$$\dot{\ell}(t)n(t) + \ell(t)\dot{n}(t) + \int_0^{\infty} x\dot{G}(x,t)dx = 0. \qquad (11)$$

The second term is then transformed by using Eq. (7), with Eq. (9),

$$\ell(t)\dot{n}(t) = -\ell(t)R\int_{\ell(t)}^{\infty} dx[x-\ell(t)]G(x,t) + 2\ell(t)R\int_{0}^{\infty} dx\int_{x+\ell(t)}^{\infty} dy\, G(y,t) + \ell(t)\dot{\ell}(t)\int_{0}^{\infty} dx\frac{\partial G(x,t)}{\partial x} = -\ell(t)\dot{\ell}(t)G(0,t) + \ell(t)R\int_{\ell(t)}^{\infty} dx[x-\ell(t)]G(x,t). \tag{12}$$

The second form was obtained by integration by parts. The last term in Eq. (11) can be transformed in the same way,

$$\int_{0}^{\infty} x\dot{G}(x,t)dx = -\ell(t)R\int_{\ell(t)}^{\infty} dx[x-\ell(t)]G(x,t) - \dot{\ell}(t)n(t). \tag{13}$$

Equations (11)–(13) combine to yield

$$\ell(t)\dot{\ell}(t)G(0,t) = 0. \tag{14}$$

For shrinking segments, $\dot{\ell}<0$, of nonvanishing length, we are thus led to our main conclusion,

$$G(0,t) = 0, \tag{15}$$

except perhaps in the limit $t\to\infty$ (in which $\dot{\ell}$ vanishes). This result indicates that the correlation hole for finite times at $x=0$ is generic for the shrinking-segment RSA, no matter how fast is the deposition kinetics that tends to "fill the hole" in the distribution at small x: The presence of the correlation hole (the depletion of the gap distribution near $x=0$) follows from the boundary condition established for $x=0$.

C. Properties of the gap-length distribution

For ordinary 1D RSA of segments of fixed length $\ell(t)=\ell\equiv\ell(\infty)$, Fig. 6 illustrates the exact solution [53] for several times and in the limit $t\to\infty$. Specifically, the gap distribution has a finite value at $x=0$, consistent with Eq. (14) for $\dot{\ell}=0$. This value actually diverges in the $t\to\infty$ limit, while a logarithmic singularity develops near $x=0$. This suggests that ordinary RSA is actually a rather singular limit of the more general shrinking-segment RSA. Indeed, the point $x=\ell(t)$ corresponds to discontinuity in the first, deposition term in the kinetic equation, Eq. (9). As a result, the fixed-ℓ RSA gap distribution has a discontinuous derivative at $x=\ell$, which becomes an actual discontinuity (jump) in the $t\to\infty$ limit. On the other hand, with segment shrinking allowed, the distribution is apparently continuous and smooth (as numerically observed), and likely analytic at all points internal to the domain of definition, $0<x<\infty$, of the gap distribution. Adding the segment-shrinkage process seems to smooth the singularities out for finite times (see Fig. 5). In terms of the kinetic equation, this is a consequence of the added third, $\sim\partial G/\partial x$ term playing the role of the "diffusive" (second-derivative) smoothing contribution with respect to the x-dependent integral (the second term). This diffusive property of the kinetic equation suggests that the function $G(x,t)$ has no singularities for any $x>0$ for finite time, though in the limit $t\to\infty$ [when $\dot{\ell}(t)\to 0$] the divergence as $x\to 0^+$ and the discontinuity at $x=\ell(\infty)$ are asymptotically restored.

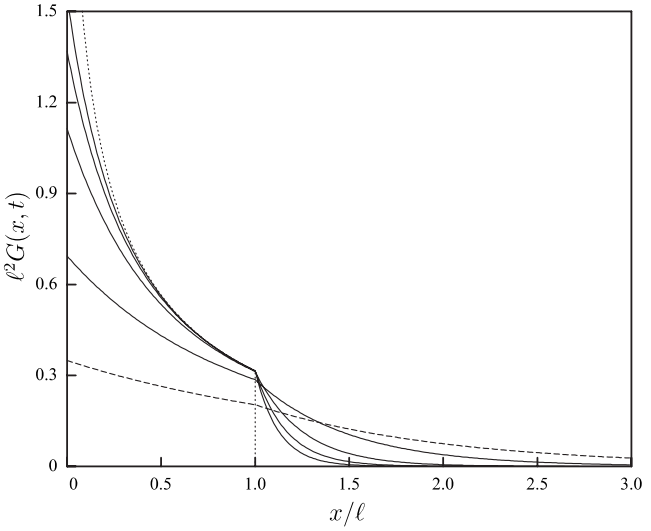

FIG. 6. Time evolution of the dimensionless gap-size distribution function $\ell^2 G(x,t)$ for segments of constant length ℓ. The dashed line corresponds to $t=\tau$. The solid lines correspond to $t=2\tau$, 4τ, 6τ, and 8τ, with increasing peak values at $x=0$, increasing values at $x=\ell$, and with respectively smaller values for $x\gg\ell$. The dotted line corresponds to $t\to\infty$, with the values for $x>\ell$ equal 0 in this limit.

The exact solution technique for the constant-length case [53] involves the use of the exponential-in-x *Ansatz* for $G(x,t)$ for $x>\ell$, recently detailed in applications for related models in [27,28], and then solution of the $x<\ell$ equation, Eq. (9), which becomes tractable because the first term is not present, whereas the integration in the second term involves a simple exponential integrand. Thus, this approach by its nature yields discontinuities if not in the function then in its first- or possibly higher-order derivatives. Attempts to use this approach, as well as more complicated, exponential-multiplied-by-polynomial *Ansätze* for $x>\ell(t)$, for time-dependent $\ell(t)$ yield solutions which satisfy the equation but possess unphysical discontinuities. Specifically, $G(x\to\ell(t)^+,t)>G(x\to\ell(t)^-,t)$ for finite times. As argued in the preceding discussion, based on heuristic considerations and confirmed by numerical results, for nonzero $\dot{\ell}(t)$ we actually expect the function $G(x,t)$ to be continuous at $x=\ell(t)$ and have all its derivatives continuous. Thus, we consider it unlikely that the shrinking-segment RSA problem in 1D can be solved exactly by the presently known techniques.

Finally, let us consider the extent to which our numerical data can confirm the restoration of the logarithmic singularity near $x=0$ in the $t\to\infty$ limit. As in 2D, our data are not accurate enough to confirm the form of the x dependence of the expected logarithmic divergence for $x\ll\ell(\infty)$, i.e., $G(x,\infty)\propto -\ln[x/\ell(\infty)]$. Regarding the t dependence, Fig. 7

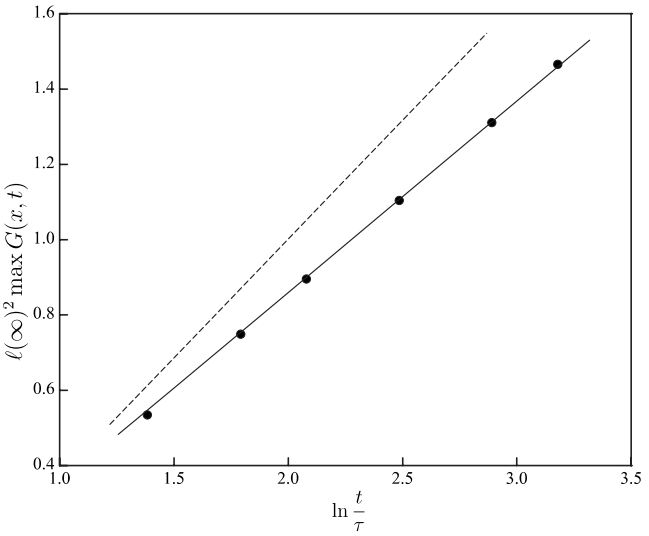

FIG. 7. The dashed straight line is the asymptotic large-time form of the gap-distribution function for the fixed-segment-length RSA; its slope is $2e^{-2\gamma}$ [see Eq. (16)]. The solid straight line is a fit of our data (shown as symbols) for $t \geqslant 4\tau$, for shrinking-segment RSA, with the estimated slope of 0.51 ± 0.02.

shows our 1D data for the peak values at small positive x (see Fig. 5), as well as the asymptotic large-time form of the exact solution peak values at $x=0$ for constant $\ell=\ell(\infty)$, the latter given by the relation [53]

$$\ell^2 G(0,t) \simeq 2e^{-2\gamma} \ln(t/\tau), \quad t \gg \tau, \tag{16}$$

where $\gamma=0.577\,215\,664\,9\ldots$ is Euler's gamma constant. Typical for data fits for logarithmic dependences, the estimated slope given in Fig. 7 may gradually drift as the t variable varies over many decades. It is possible that it reaches the larger value of the fixed-segment RSA: We consider the error estimate, 0.02, here and in the 2D case (Fig. 3) inconclusive.

In summary, we investigated a RSA model in which deposition of arriving objects, which tends to form small gaps or voids, competes with the process of shrinking of the objects, both those already deposited and those newly arriving. The latter process always "wins" at finite time, and as a result a correlation hole opens up in the correlation properties considered. In fact, analytical considerations in 1D suggest that this property is generic for an initially empty substrate. The numerical Monte Carlo results reported support this conclusion for the time dependences studied. For the exponential-decay time dependence of the object sizes studied in 1D and 2D, we also found preliminary evidence that logarithmic divergence of the correlation properties at contact is restored as $t \to \infty$. For 1D, the discontinuous behavior of the gap distribution at $x=\ell(\infty)$ also reemerges in this limit.

ACKNOWLEDGMENTS

The authors thank Dr. S. Minko and Dr. I. Tokarev for instructive discussions, and acknowledge support of this research by the NSF under Grant No. DMR-0509104.

[1] See J. W. Evans, Rev. Mod. Phys. **65**, 1281 (1993), for a review.
[2] See M. C. Bartelt and V. Privman, Int. J. Mod. Phys. B **5**, 2883 (1991), for a review.
[3] *Adhesion of Submicron Particles on Solid Surfaces*, edited by V. Privman, Colloids Surf., A **165**, 1 (2000) (a collection of review articles).
[4] *Nonequilibrium Statistical Mechanics in One Dimension*, edited by V. Privman (Cambridge University Press, Cambridge, U.K., 1997) (a collection of review articles).
[5] See J. J. Ramsden, Chem. Soc. Rev. **24**, 73 (1995), for a review.
[6] P. R. Van Tassel, P. Viot, and G. Tarjus, J. Chem. Phys. **106**, 761 (1997).
[7] S. Torquato, O. U. Uche, and F. H. Stillinger, Phys. Rev. E **74**, 061308 (2006).
[8] A. V. Subashiev and S. Luryi, Phys. Rev. E **75**, 011123 (2007).
[9] See V. Privman, J. Adhes. **74**, 421 (2000), for a review.
[10] W. van Roosbroeck, Phys. Rev. **139**, A1702 (1965).
[11] R. C. Alig, S. Bloom, and C. W. Struck, Phys. Rev. B **22**, 5565 (1980).
[12] M. Inoue, Phys. Rev. B **25**, 3856 (1982).
[13] P. Viot, G. Tarjus, and J. Talbot, Phys. Rev. E **48**, 480 (1993).
[14] J.-S. Wang, P. Nielaba, and V. Privman, Physica A **199**, 527 (1993).
[15] D. Boyer, J. Talbot, G. Tarjus, P. Van Tassel, and P. Viot, Phys. Rev. E **49**, 5525 (1994).
[16] Z. Adamczyk and P. Warszyński, Adv. Colloid Interface Sci. **63**, 41 (1996).
[17] G. J. Rodgers and Z. Tavassoli, Phys. Lett. A **246**, 252 (1998).
[18] M. K. Hassan, J. Schmidt, B. Blasius, and J. Kurths, Phys. Rev. E **65**, 045103(R) (2002).
[19] D. J. Burridge and Y. Mao, Phys. Rev. E **69**, 037102 (2004).
[20] N. A. M. Araújo and A. Cadilhe, Phys. Rev. E **73**, 051602 (2006).
[21] P. Nielaba and V. Privman, Mod. Phys. Lett. B **6**, 533 (1992).
[22] J.-S. Wang, P. Nielaba, and V. Privman, Mod. Phys. Lett. B **7**, 189 (1993).
[23] M. C. Bartelt and V. Privman, Phys. Rev. A **44**, R2227 (1991).
[24] A. Cadilhe, N. A. M. Araújo, and V. Privman, J. Phys.: Condens. Matter **19**, 065124 (2007).
[25] N. A. M. Araújo, A. Cadilhe, and V. Privman, Phys. Rev. E **77**, 031603 (2008).
[26] V. Privman and P. Nielaba, Europhys. Lett. **18**, 673 (1992).
[27] E. Ben-Naim and P. L. Krapivsky, Phys. Rev. E **54**, 3562 (1996).
[28] O. Gromenko, V. Privman, and M. L. Glasser, J. Comput. Theor. Nanosci. **5**, 2119 (2008).
[29] V. Privman, Europhys. Lett. **23**, 341 (1993).
[30] N. V. Dziomkina and G. J. Vancso, Soft Matter **1**, 265 (2005).
[31] J. A. Liddle, Y. Cui, and P. Alivisatos, J. Vac. Sci. Technol. B **22**, 3409 (2004).

[32] T. Ogawa, Y. Takahashi, H. Yang, K. Kimura, M. Sakurai, and M. Takahashi, Nanotechnology **17**, 5539 (2006).
[33] R. D. Deshmukh, G. A. Buxton, N. Clarke, and R. J. Composto, Macromolecules **40**, 6316 (2007).
[34] R. Lupitskyy, M. Motornov, and S. Minko, Langmuir **24**, 8976 (2008).
[35] M. Motornov, R. Sheparovych, R. Lupitskyy, E. MacWilliams, and S. Minko, J. Colloid Interface Sci. **310**, 481 (2007).
[36] N. Nath and A. J. Chilkoti, J. Am. Chem. Soc. **123**, 8197 (2001).
[37] I. Tokareva, S. Minko, J. H. Fendler, and E. Hutter, J. Am. Chem. Soc. **126**, 15950 (2004).
[38] Z. Y. Zhong, S. Patskovskyy, P. Bouvrette, J. H. T. Luong, and A. Gedanken, J. Phys. Chem. B **108**, 4046 (2004).
[39] S. Lee and V. H. Pérez-Luna, Anal. Chem. **77**, 7204 (2005).
[40] I. Tokareva, I. Tokarev, S. Minko, E. Hutter, and J. H. Fendler, Chem. Commun. (Cambridge) **2006**, 3343.
[41] O. Azzaroni, A. A. Brown, N. Cheng, A. Wei, A. M. Jonas, and W. T. S. Huck, J. Mater. Chem. **17**, 3433 (2007).
[42] Y. Ding, X. H. Xia, and H. S. Zhai, Chem.-Eur. J. **13**, 4197 (2007).
[43] Y. Pomeau, J. Phys. A **13**, L193 (1980).
[44] R. H. Swendsen, Phys. Rev. A **24**, 504 (1981).
[45] A. Yethiraj, C. K. Hall, and K. G. Honnell, J. Chem. Phys. **93**, 4453 (1990).
[46] Y. C. Chiew, J. Chem. Phys. **93**, 5067 (1990).
[47] E. Kierlik and M. L. Rosinberg, J. Chem. Phys. **99**, 3950 (1993).
[48] J. Huh, O. Ikkala, and G. ten Brinke, Macromolecules **30**, 1828 (1997).
[49] V. Krakoviack, E. Kierlik, M.-L. Rosinberg, and G. Tarjus, J. Chem. Phys. **115**, 11289 (2001).
[50] *Strongly Coupled Coulomb Systems*, edited by G. J. Kalman, J. M. Rommel, and K. Blagoev (Springer, New York, 2002).
[51] J. Feder, J. Theor. Biol. **87**, 237 (1980).
[52] J.-S. Wang, Int. J. Mod. Phys. C **5**, 707 (1994).
[53] J. J. González, P. C. Hemmer, and J. S. Høye, Chem. Phys. **3**, 228 (1974).